

Coupling strength of complex plasmonic structures in the multiple dipole approximation

Lutz Langguth and Harald Giessen*

*4th Physics Institute and Research Center SCOPE, University of Stuttgart,
70550 Stuttgart, Germany*

**giessen@physik.uni-stuttgart.de*

Abstract: We present a simple model to calculate the spatial dependence of the interaction strength between two plasmonic objects. Our approach is based on a multiple dipole approximation and utilizes the current distributions at the resonances in single objects. To obtain the interaction strength, we compute the potential energy of discrete weighted dipoles associated with the current distributions of the plasmonic modes in the scattered fields of their mutual partners. We investigate in detail coupled stacked plasmonic wires, stereometamaterials and plasmon-induced transparency materials. Our calculation scheme includes retardation and can be carried out in seconds on a standard PC.

© 2011 Optical Society of America

OCIS codes: (250.5403) Plasmonics; (350.4238) Nanophotonics and photonic crystals; (160.3918) Metamaterials.

References and links

1. C. Dahmen, B. Schmidt, and G. von Plessen, "Radiation damping in metal nanoparticle pairs," *Nano Lett.* **7**, 318–322 (2007).
2. N. Liu, H. Guo, L. Fu, S. Kaiser, H. Schweizer, and H. Giessen, "Plasmon hybridization in stacked cut-wire metamaterials," *Adv. Mater.* **19**, 3628–3632 (2007).
3. B. Lamprecht, G. Schider, R. T. Lechner, H. Ditlbacher, J. R. Krenn, A. Leitner, and F. R. Aussenegg, "Metal nanoparticle gratings: influence of dipolar particle interaction on the plasmon resonance," *Phys. Rev. Lett.* **84**, 4721–4724 (2000).
4. S.-C. Yang, H. Kobori, C.-L. He, M.-H. Lin, H.-Y. Chen, C. Li, M. Kanehara, T. Teranishi, and S. Gwo, "Plasmon hybridization in individual gold nanocrystal dimers: direct observation of bright and dark modes," *Nano Lett.* **10**, 632–637 (2010).
5. S. Linden, C. Enkrich, M. Wegener, J. Zhou, T. Koschny, and C. M. Soukoulis, "Magnetic response of metamaterials at 100 terahertz," *Science* **306**, 1351–1353 (2004).
6. N. Liu and H. Giessen "Coupling effects in optical metamaterials," *Angew. Chem., Int. Ed.* **49**, 9838–9852 (2010).
7. M. Kafesaki, T. Koschny, R. S. Penciu, T. F. Gundogdu, E. N. Economou, and C. M. Soukoulis, "Left-handed metamaterials: detailed numerical studies of the transmission properties," *J. Opt. A* **7**, S12–S22 (2005).
8. V. M. Shalaev, "Optical negative-index metamaterials," *Nat. Photonics* **1**, 41–48 (2007).
9. N. Liu, H. Guo, L. Fu, S. Kaiser, H. Schweizer, and H. Giessen, "Three-dimensional photonic metamaterials at optical frequencies," *Nat. Mater.* **7**, 31–37 (2008).
10. N. Liu, H. Liu, S. Zhu, and H. Giessen, "Stereometamaterials," *Nat. Photonics* **3**, 157–162 (2009).
11. D. A. Powell, K. Hannam, I. V. Shadrivov, Y. S. Kivshar, "Near-field interaction of twisted splitting resonators," *Phys. Rev. B* **83**, 235420 (2011).

12. N. Liu, L. Langguth, T. Weiss, J. Kästel, M. Fleischhauer, T. Pfau, and H. Giessen, "Plasmonic analogue of electromagnetically induced transparency at the Drude damping limit," *Nat. Mater.* **8**, 758–762 (2009).
13. S. Zhang, D. A. Genov, Y. Wang, M. Liu, and X. Zhang, "Plasmon-induced transparency in metamaterials," *Phys. Rev. Lett.* **101**, 047401 (2008).
14. N. Verellen, Y. Sonnefraud, H. Sobhani, F. Hao, V. V. Moshchalkov, P. Van Dorpe, P. Nordlander, and S. A. Maier, "Fano resonances in individual coherent plasmonic nanocavities," *Nano Lett.* **9**, 1663–1667 (2009).
15. M. Hentschel, M. Saliba, R. Vogelgesang, H. Giessen, A. P. Alivisatos, and N. Liu, "Transition from isolated to collective modes in plasmonic oligomers," *Nano Lett.* **10**, 2721–2726 (2010).
16. J. Fan, C. Wu, K. Bao, J. Bao, R. Bardhan, N. J. Halas, V. N. Manoharan, P. Nordlander, G. Shvets, and F. Capasso, "Self-assembled plasmonic nanoparticle clusters," *Science* **328**, 1135–1138 (2010).
17. J. B. Lassiter, H. Sobhani, J. A. Fan, J. Kundu, F. Capasso, P. Nordlander, and N. J. Halas, "Fano resonances in plasmonic nanoclusters: geometrical and chemical tunability," *Nano Lett.* **10**, 3184–3189 (2010).
18. H. Liu, J. X. Cao, and S. N. Zhu, "Lagrange model for the chiral optical properties of stereometamaterials," *Phys. Rev. B* **81**, 241403 (2010).
19. B. Luk'yanchuk, N. I. Zheludev, S. A. Maier, N. J. Halas, P. Nordlander, H. Giessen, and C. T. Chong, "The Fano resonance in plasmonic nanostructures and metamaterials," *Nat. Mater.* **9**, 707–715 (2010).
20. N. Liu, M. Mesch, T. Weiss, M. Hentschel, and H. Giessen, "Infrared perfect absorber and its application as plasmonic sensor," *Nano Lett.* **10**, 2342–2348 (2010).
21. E. Prodan and P. Nordlander, "Plasmon hybridization in spherical nanoparticles," *J. Chem. Phys.* **120**, 5444–5454 (2004).
22. E. Prodan, C. Radloff, N. J. Halas, and P. Nordlander, "A hybridization model for the plasmon response of complex nanostructures," *Science* **302**, 419–422 (2003).
23. P. Nordlander, C. Oubre, E. Prodan, K. Li, and M. I. Stockman, "Plasmon hybridization in nanoparticle dimers," *Nano Lett.* **4**, 899–903 (2004).
24. T. J. Davis, D. E. Gomez, and K. C. Vernon, "Simple model for the hybridization of surface plasmon resonances in metallic nanoparticles," *Nano Lett.* **10**, 2618–2625 (2010).
25. I. Sersic, C. Tuambilangana, T. Kampfrath, and A. F. Koenderink, "Magneto-electric point scattering theory for metamaterial scatterers," *Phys. Rev. B* **83**, 245102 (2011).
26. C. Rockstuhl, F. Lederer, C. Etrich, T. Zentgraf, J. Kuhl, and H. Giessen, "On the reinterpretation of resonances in split-ring-resonators at normal incidence," *Opt. Express* **14**, 8827–8836 (2006).
27. J. Dorfmueller, R. Vogelgesang, W. Khunsin, C. Rockstuhl, C. Etrich, and K. Kern, "Plasmonic nanowire antennas: experiment, simulation, and theory," *Nano Lett.* **10**, 3596–3603 (2010).
28. J. Dorfmueller, R. Vogelgesang, R. T. Weitz, C. Rockstuhl, C. Etrich, T. Pertsch, F. Lederer, and K. Kern, "Fabry-Pérot resonances in one-dimensional plasmonic nanostructures," *Nano Lett.* **9**, 2372–2377 (2009).
29. T. Meyrath, T. Zentgraf, and H. Giessen, "Lorentz model for metamaterials: optical frequency resonance circuits," *Phys. Rev. B* **75**, 205102 (2007).
30. CST, CST Microwave Studio (2009).
31. C. L. Garrido Alzar, M. A. G. Martinez, and P. Nussenzeig, "Classical analog of electromagnetically induced transparency," *Am. J. Phys.* **70**, 37 (2002).
32. J. K. Gansel, M. Thiel, M. S. Rill, M. Decker, K. Bade, V. Saile, G. von Freymann, S. Linden, and M. Wegener, "Gold helix photonic metamaterial as broadband circular polarizer," *Science* **325**, 1513–1515 (2009).
33. N. Liu, M. Hentschel, Th. Weiss, A. P. Alivisatos, and H. Giessen, "Three-dimensional plasmon rulers," *Science* **332**, 1407–1410 (2011).

1. Introduction

The interaction of plasmonic objects has currently generated substantial scientific interest. Very often, elements such as nanospheres, nanodiscs, cut-wires, etc., have been investigated [1–4]. Recently, the field of metamaterials has exploited also more complex shapes of plasmonic objects, such as split-ring resonators [5, 6], cut-wire pairs [7, 8], stacked split-ring systems [9–11], combinations of cut-wire pairs and single nanowires [12, 13], nanodots and nanorings [14], as well as plasmonic oligomers [15–17].

Interaction between the individual plasmonic nanoobjects plays the key role for the

understanding of the optical properties of the collective system. This is especially true for the new field of plasmonic metamaterials, where not only electric dipole interaction plays the main role, but also magnetic interaction as well as higher order electric multipoles can have substantial influence. One prominent example for such a system are stereometamaterials [10], which can exhibit strong chiral optical properties [18]. Dipole-quadrupole coupling is also the key mechanism for generation of ultranarrow resonances in the optical spectrum of plasmonic objects, which arise from Fano interference [19]. Such plasmonic analogs of electromagnetically induced transparency have led to novel sensors with extremely high figures of merit [20]. Common to all of these examples is the importance of coupling between the plasmonic elements. Simple systems, such as dimers consisting of nanospheres, can be treated analytically. Dimers made from plasmonic nanoshells are also well behaved and have been described using the plasmon hybridization picture [21,22]. Often, the interaction is observable through a resonance shift or resonance splitting in the optical spectra.

When it comes to more complex systems, the interaction between the individual constituents is yet not easily understood. The optical response of coupled structures can nowadays be computed with numerical methods which solve the full Maxwell equations (such as FDTD, Fourier Modal Methods, MMP and Finite Integral Methods), but the obtained spectra need careful interpretation. In order to gain some insight into the distance dependence of the coupling strength, it is possible to analyze the resonance shift or mode-splitting in the spectrum [23]. However the splitting needs to be large enough to be recognizable (i.e., the splitting of the resonances needs to be larger than its full width at half maximum) and for each spatial configuration the whole spectrum has to be computed. For complex structures, large calculation volumes, or a systematic search in parameter space of relative spatial arrangements, the use of full Maxwell solvers is not convenient or not feasible because of the required computational effort. Such knowledge about distance-dependent coupling strength might, however, be the key for the design of novel plasmonic devices. One example is sensors, where the coupling determines the lineshape and, hence, the sensitivity of the sensor. Appropriate fabrication parameters and tolerances need to be known, and, therefore, the proper know-how of the coupling is of crucial importance. A different path to understand the interaction between plasmonic objects is to model the interplay of the (two) objects analytically. Up to now, mostly electrostatic models [24] or point-dipole models [25] have been applied to explain the spatial dependence of the interplay between nano-objects. Electrostatic models break down when the distances between the objects exceed a quarter of the effective wavelength, whereas point-dipole models fails to model the nearfields of extended structures correctly and therefore break down at small distances.

We present a simple model that uses independently calculated currents inside each structure at each resonance and then computes the spatial dependence of interaction strength. The required resonance positions of each structure and the corresponding current distributions can easily and efficiently be calculated with available Maxwell solvers. Note that the absolute coupling strength cannot be computed with this method and the total amplitude is fitted to the reference.

1.1. Modes in plasmonic systems

Each plasmonic object exhibits resonances. Their energies and lifetimes are determined by the geometric shape, material, and dielectric environment [26]. For thin metallic wires, simple models can describe the current distribution for different modes. We assume the currents in metallic nano-wires to flow on a line on the wire axis, forming

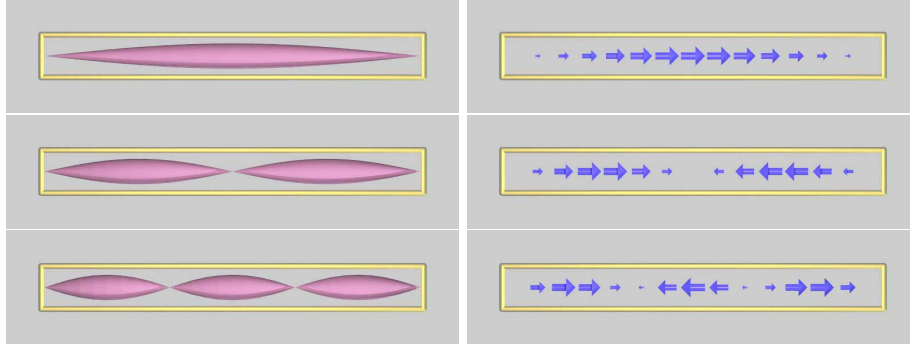


Fig. 1. Schematic current distributions in a plasmonic wire for the first three eigenmodes (from top to bottom).

standing waves for the different modes (Fig. 1, left side). In a first approximation, the currents have nodes exactly at the geometric end of the wire, which is not strictly true [27, 28].

Furthermore, we discretize the currents along the wire axis into point currents with a sinusoidal amplitude modulation A_i of a standing wave (Fig.1, right side) [29]. The point current flowing forth and back constitutes an oscillating electric point dipole \vec{p} with the radiation pattern expressed in Eq. (1):

$$\vec{E}_{DD}(\vec{r}, \vec{p}) = \frac{1}{4\pi\epsilon_0} \left\{ \frac{\omega^2}{c^2 r} \hat{r} \times \vec{p} \times \hat{r} + \left(\frac{1}{r^3} - \frac{i\omega}{cr^2} \right) \left[3\hat{r}(\hat{r} \cdot \vec{p}) - \vec{p} \right] \right\} e^{i\omega r/c}. \quad (1)$$

Summing up the electric fields of all discrete dipoles of the object (Eq. (2)) gives us a good approximation for the scattered field of the nanoparticle at the resonance:

$$\vec{E}_{\text{scat},1}(\vec{r}) = \sum_{i=1}^N A_i \vec{E}_{DD}(\vec{r}_i - \vec{r}, \vec{p}_i). \quad (2)$$

In the static case, the work of a current in an external field is given by $U = -\vec{E} \cdot \vec{j}$. For the time-harmonic case the cycle-averaged potential energy U for a point-current dipole \vec{p}_2 in an external field \vec{E} can be written as in Eq. (3)

$$U = -\frac{\pi}{\omega} \text{Re} \left\{ \vec{E}(\vec{r}_2) \cdot \vec{p}_2^* \right\}. \quad (3)$$

For two extended objects, we also discretize the current distribution in the second object into a set of oscillating dipole moments $\vec{p}_{2,j}$ and then calculate the scalar product of the scattered field of object one, $\vec{E}_{\text{scat},1}$, with the discretized currents of object two (Eq. (4)):

$$U = -\frac{\pi}{\omega} \text{Re} \left\{ \sum_{j=1}^N \vec{E}_{\text{scat},1}(\vec{r}_j) \cdot \vec{p}_{2,j}^* \right\}. \quad (4)$$

The calculated potential energy U is then proportional to the coupling strength of the system at one specific frequency ω . Due to the efficient calculation of U , the number of dipoles can easily be increased until convergence is reached.

1.2. Relative phase between two coupled particle plasmons

One particle plasmon, driven by an external time-harmonic field will oscillate with a specific phase delay such that the charges and currents of the plasmon exhibit an extremum of potential energy in the incident light field.

In the presence of two particle plasmons in an arrangement such that only one is excited by the external field, the second one can only be excited by the scattered field of the first one. In this configuration, the phase delay of particle plasmon two will be such that it exhibits an extremum of its potential energy in the scattered field of particle plasmon one. In our model we calculate via simple algebra for which phase difference φ of $\vec{E}_{\text{scat},1}$ and \vec{p}_2 the complex scalar $\sum_{j=1}^N \vec{E}_{\text{scat},1}(\vec{r}_j) \cdot \vec{p}_{2,j}^*$ becomes real. Changing the relative phase by φ , Eq. (4) yields an extremal interaction energy U .

In the following, we are going to present two cases, namely two perpendicularly stacked cut wires and a dipole-quadrupole-coupled complex stacked plasmonic structure. The condition is not fulfilled in the third system which we discuss below, namely a stereometamaterial consisting of two stacked and twisted split-ring resonators. The reason is that in this case both objects are driven by the external light field. However due to the short distances and the field enhancement near the structures, the interaction is dominated by near field coupling, and the external field can be neglected in first order.

2. Structures

In order to examine the validity of our model, we examined our coupling model with three different geometries. Our first system is a stacked and perpendicularly oriented cut-wire pair. Our second system is a more complex system which consists of three plasmonic wires, which constitute a quadrupole-dipole coupled system, and our third system is a stereometamaterial consisting of two stacked split-ring resonators. The systems include different levels of coupling, namely electric coupling in the near- as well as in the far-field, coupling of fundamental modes to higher-order multipoles, as well as electric and magnetic coupling.

2.1. Perpendicular cut wire pair

The first and simplest system that we are going to examine are two stacked gold cut-wires of equal size and geometry (length 400 nm, width and height 40 nm) in vacuum ($n = 1$). One wire is aligned along the x axis and the other is aligned along the y-axis and hence perpendicular to the first one (see Fig. 2a).

They are arranged in such a way that they have one common x-y coordinate at their respective ends. We vary the z-distance from 50 nm center to center distance up to 400 nm between both objects and analyze their mutual coupling. First we have calculated the response of this system with a commercial finite-integration time domain (FITD) algorithm software [30] and extracted the spectral splitting from the resulting spectra (see Fig. 2b). The spectral splitting is plotted as squares in Fig. 3a. At a center-to-center distance of $d_z = 300$ nm the splitting becomes smaller than half the linewidth of the resonance and hence could not be extracted anymore from the spectrum.

Assuming an incident field polarized parallel to the first wire, the second one cannot be excited directly from the incident field at the resonant frequency and, therefore, can only be excited by the scattered light of wire 1. We discretized the fundamental plasmon mode in the wire [26] into N dipoles as described above and calculated the interaction energy at the resonance at $\nu = 200$ THz using our model. The coupling results for $N = 1, 3, 5, 9$ and 15 discrete dipoles with their amplitude set to the appropriate value which we obtained from the respective fundamental plasmon mode are plotted in Fig.

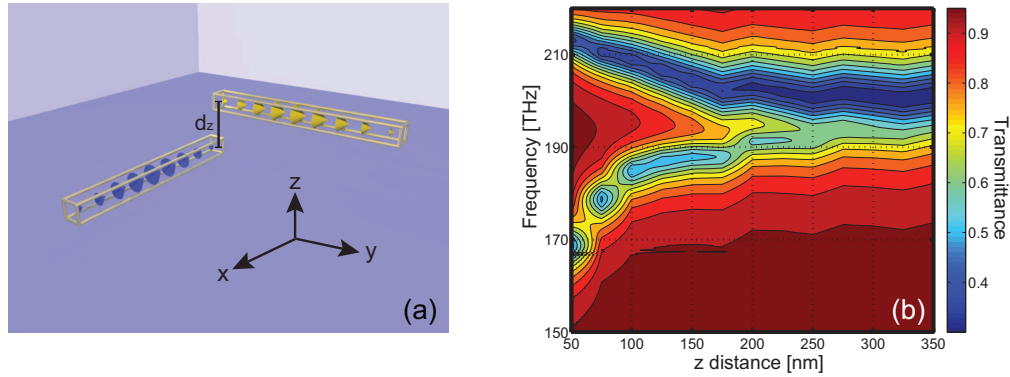


Fig. 2. a) Geometry of the system and the discretized currents. b) Contour of transmittance spectra (Finite-integral time domain simulation [30]).

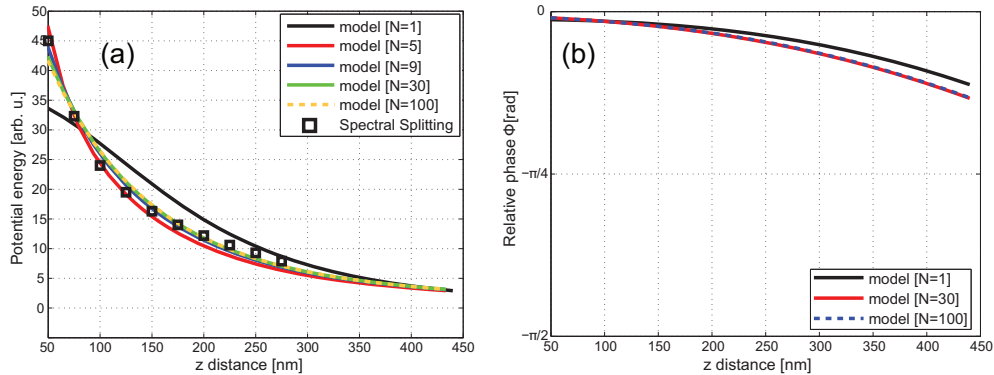


Fig. 3. a) Coupling strength in dependence of z-distance. b) Relative phase ϕ as function of z distance.

3a as solid line. Already for a discretization level of $N = 9$ dipoles (blue curve) the agreement of our model with the full Maxwell simulations is excellent. Figure 3b shows the phase shift between the modes in the top and bottom wires, which is more or less flat at $\phi \approx 0$ degrees for these wire separations.

We are going to inspect now the situation upon larger distances, where retardation between the two wires is no longer negligible. Hence, we vary the distance from 0 to 3000 nm, i.e., more than two resonance wavelengths of the nanowire system.

Figure 4a depicts the model calculation for these large distances, which show a decreasing coupling. The values are hard to extract from the FITD simulations, as the splitting is no longer visible due to the width of the individual resonances. The phase evolves after the initial curved behavior into a linear shape, as expected from pure retardation.

2.2. Dipole-quadrupole structure

The second configuration is a coupled system of three plasmonic wires (see Fig. 5b) embedded in a dielectric environment ($n = 1.55$). Two of them are in the lower plane and have a length of 315 nm. They are laterally separated by a distance (center to center) of

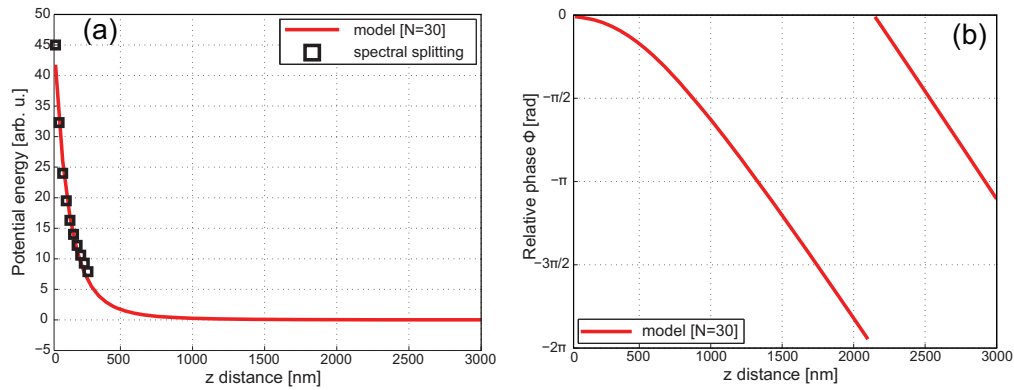


Fig. 4. a) Coupling strength for long distances: the extraction of the mode splitting from FITD-simulations was only possible up to 300 nm. b) Linear scaling of the relative phase between the currents for long distances shows the effect of retardation.

300 nm. Above them is a single gold nanowire of length 355 nm which is perpendicular to the bottom wires. All three wires have a width of 80 nm and height of 40 nm, the stacking distance in z -direction is 70 nm. The system resembles a plasmonic analog of electromagnetically induced transparency (EIT) [12]. The single top nanowire represents a plasmonic dipole, and the two wires below constitute a plasmonic quadrupole. Upon excitation with light at its resonance at $\lambda_{vac} = 1.66 \mu\text{m}$ that is polarized in the x -direction (the direction of the long axis of the top nanowire), the dipole is excited. By near-field coupling, the dark quadrupolar mode of the lower wires (which is not excited by the incoming light) is excited. A peculiarity of this EIT system is the fact that the excitation of the quadrupole takes only place if the dipole is laterally shifted away from the symmetry axis of the quadrupole by a shift s (see Fig. 5a). The *experimental* transmittance spectra from reference [12] for different lateral shifts s are shown in Fig. 5c. In order to extract the coupling strength between the dipole and the quadrupole in dependence on this parameter s , a fit of the experimental spectra to a classical EIT model [31] was carried out and plotted as squares in Fig. 6a. In order to understand the coupling strength behavior upon lateral shift s , we discretized the currents in the three wires in a similar fashion as above. Again, sinusoidal modes in each single wire have been assumed. The solid line in Fig. 6a shows the resulting coupling strength for different numbers of discretized dipoles. The coupling strength behaves more or less linearly with lateral shift for small values of s , and saturates when the position of the dipole bar approaches the edges of the quadrupole bars underneath. A single dipole per wire can already describe the initial linear behavior. We determine that a number of $N = 30$ (green curve) gives a quite good agreement between our simple model and the experiment for larger lateral shifts as well, and convergence has been achieved. The extremal condition described above in section 1.2 leads to the phase relation between the upper and lower dipole and quadrupole as plotted in Fig. 6b. The phase is more or less flat at $\phi \approx 0$ degrees for the stacking distance of 70 nm, regardless of the shift parameter s .

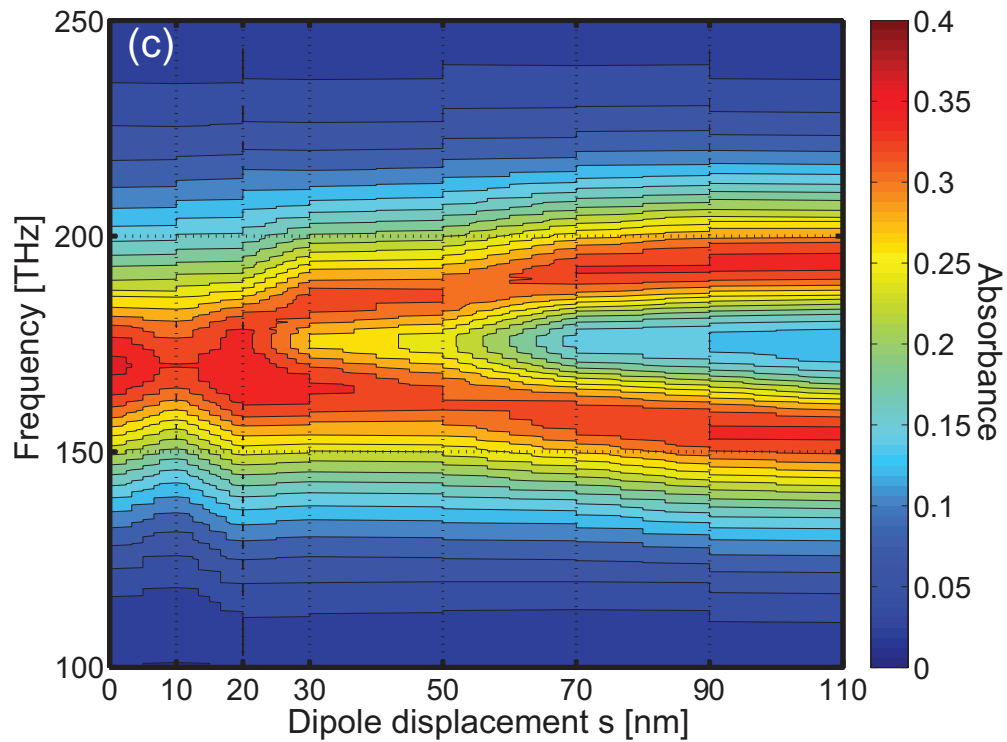
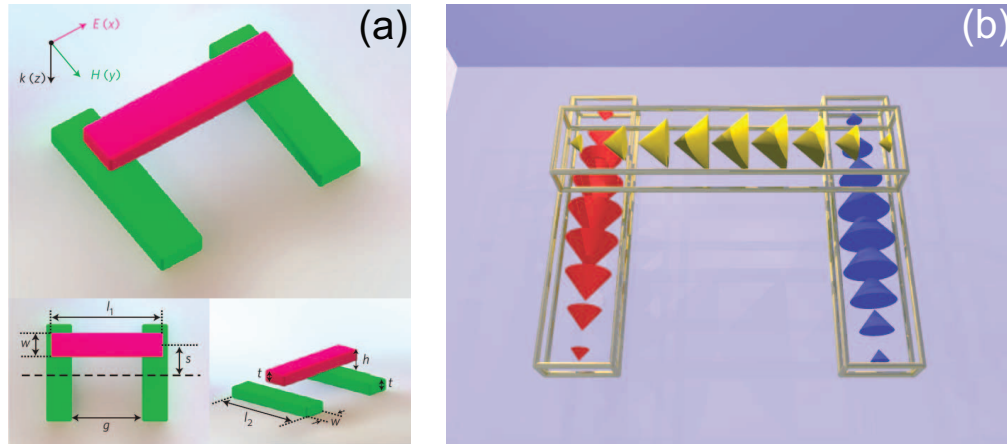


Fig. 5. a) Schematic view of the plasmonic EIT structure . b) Schematic picture of the discretized currents in the structure. The cones illustrate the 27 discrete dipoles for the calculation (9 in each wire). c) Contour plot of experimental absorbance data of the coupled dipole-quadrupole structure.

2.3. Coupled split ring resonators

The third system that we discuss here is a stereometamaterial which consists of two stacked split ring resonators of lateral size 230 nm, width 230 nm, and height 50 nm in vacuum (see [10]). The center to center vertical distance is kept constant at 100 nm.

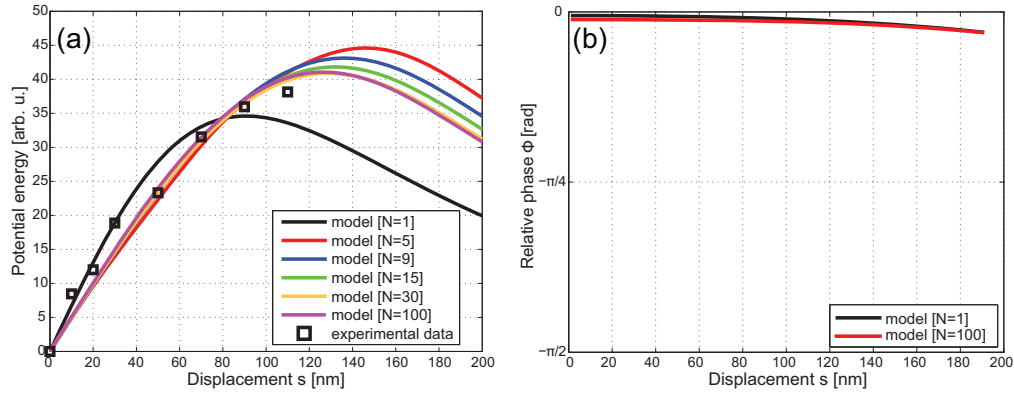


Fig. 6. a) Different number of dipoles for each wire ($N = 1, 5, 9, 15, 30, 100$) in comparison with experimental results. b) Relative phase ϕ as function of shifting parameter s .

We change the coupling between the two systems by varying the twist angle θ from 0 to 180 degrees.

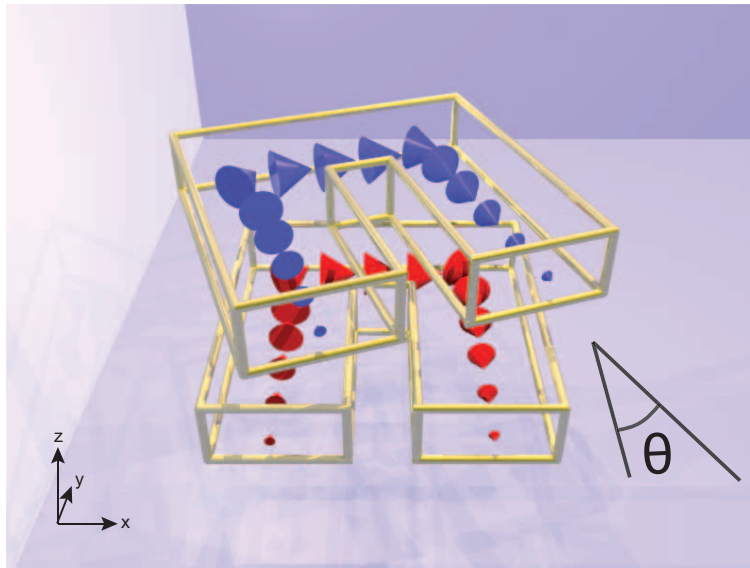


Fig. 7. Stacked twisted split ring resonators: the cones depict the discretization of the current in each split ring resonator into $N = 15$ discrete dipoles each.

Linearly polarized light which impinges from the bottom onto that sample along the gap of the lower split-ring can excite a fundamental plasmon mode between the ends of the wire [26]. The fundamental resonance occurs at a wavelength of $\lambda_{vac} = 1.5 \mu\text{m}$. Hence, a particle plasmon along the total wire with a more or less sinusoidal current distribution is excited (see Fig. 7). We treat the split ring resonator element as a wire which was bent twice [26]. We assume that the second split ring in our model is only excited by coupling to the first one. The total coupling strength is composed of dipolar and higher-order multipolar electrical modes as well as dipolar magnetic modes [18].

The spectral splitting has been extracted from the numerical extinction spectra of [10] and is plotted as squares in Fig. 8a. Our model calculation is shown for $N = 9$ up to $N = 100$. It is clear that for such a complex system, a single straight dipole cannot account for the coupling behavior upon twisting at all. We find that $N = 50$ gives already satisfactory agreement between the FITD simulation (which actually agrees quite well with experimental observations, see Liu et al. [10]) and our model. Towards $N = 100$, our model converges well. For a more complex structure we need more elementary dipoles to account for the associated modes. Our model reproduces the characteristic features of the system with a modest splitting at $\theta = 0^\circ$, a minimum at a critical angle of $\theta_c \approx 60^\circ$, and a stronger splitting at $\theta = 180^\circ$.

Using our model of extremal energies, we also retrieved the phase between the oscillators. Different from our previous two cases, the phase behavior is not flat. The retrieved phase between the top and bottom oscillators varies in our model between $\pi/5$ at $\theta = 0^\circ$ twist angle to slightly above π for $\theta = 180^\circ$ twist angle. The latter result can be easily understood, as the twist angle of 180° results in a π phase shift between the two excitations and because the distance gives only a very small retardation. This small retardation might be responsible for the small deviation of the phase to a value of π . One should mention that the interplay of external excitation and internal coupling in such a stereometamaterial is very intricate and far from being understood in a simple model system.

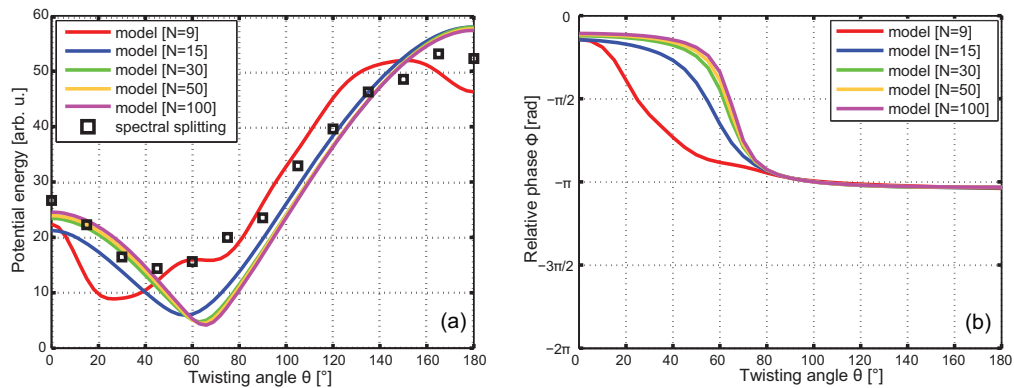


Fig. 8. a) Coupling strength in dependence of the twisting angle θ . b) Relative phaseshift as function of θ .

3. Summary/outlook

In this paper, we demonstrated how a very simple and efficient multiple dipole approximation model can account for the coupling behavior of quite complex plasmonic nanostructures. We took the modes of simple constituents of our complex nanostructures and weighted up to $N = 100$ discrete dipoles with the strength of the current. Summing then over all simple interactions between mutual dipoles and calculating the interaction energy, we were able to derive the total splitting energy of our complex systems within a computing time of less than a minute on a standard PC. We obtained very good overall agreement with much more complex FITD simulations and were even

able to calculate coupling strengths for distances where extraction from FITD data was no longer possible due to the small energy splitting. We were also able to determine the phase behavior between the individual oscillators. Retardation was taken into account in all cases. Our model with our quite simple assumptions should be able to predict the behavior of even more complex nanostructures in the near-field as well in as in the far field with very small effort. Our method can therefore facilitate parameter studies for the design of novel nanoplasmonic devices which are based on coupled structures, such as novel polarizers [32], plasmonic sensors [20] or 3D plasmon rulers [33] in the future.

Acknowledgments

We thank BMBF (3D Metamat) and DFG (SPP1391 and Open Access Publishing Grant) for support.